

# Observation of the Pairing Gap in a Strongly Interacting Fermi Gas

C. Chin,<sup>1</sup> M. Bartenstein,<sup>1</sup> A. Altmeyer,<sup>1</sup> S. Riedl,<sup>1</sup> S. Jochim,<sup>1</sup>  
J. Hecker Denschlag,<sup>1</sup> and R. Grimm<sup>1,2\*</sup>

<sup>1</sup>Institut für Experimentalphysik, Universität Innsbruck,  
Technikerstraße 25, 6020 Innsbruck, Austria

<sup>2</sup>Institut für Quantenoptik und Quanteninformation,  
Österreichische Akademie der Wissenschaften, 6020 Innsbruck, Austria

\*To whom correspondence should be addressed; E-mail: [rudolf.grimm@uibk.ac.at](mailto:rudolf.grimm@uibk.ac.at).

**We study fermionic pairing in an ultracold two-component gas of  ${}^6\text{Li}$  atoms by observing an energy gap in the radio-frequency excitation spectra. With control of the two-body interactions via a Feshbach resonance we demonstrate the dependence of the pairing gap on coupling strength, temperature, and Fermi energy. The appearance of an energy gap with moderate evaporative cooling suggests that our full evaporation brings the strongly interacting system deep into a superfluid state.**

The spectroscopic observation of a pairing gap in the 1950s marked an important experimental breakthrough in research on superconductivity (1). The gap measurements provided a key to investigate the paired nature of the particles responsible for the frictionless current in metals at very low temperatures. The ground-breaking BCS (Bardeen-Cooper-Schrieffer) theory, developed at about the same time, showed that two electrons in the degenerate Fermi sea can be coupled by an effectively attractive interaction and form a delocalized, composite particle with bosonic character. BCS theory predicted that the gap in the low-temperature limit is proportional to the critical temperature  $T_c$  for the phase transition in agreement with the experimental measurements. In general, the physics of superconductivity and superfluidity goes far beyond the weak coupling limit of BCS theory. In the limit of strong coupling, paired fermions form localized bosons and the system can undergo Bose-Einstein condensation (BEC). The BCS limit and the BEC limit are connected by a smooth BCS-BEC crossover, which has been subject of great theoretical interest for more than three decades (2, 3, 4, 5). The formation of pairs generally represents a key ingredient of superfluidity in fermionic systems and the gap energy is a central quantity to characterize pairing regime.

The rapid progress in experiments with ultracold degenerate Fermi gases (6) has opened up a unique test ground to study phenomena related to pairing and superfluidity at densities typically a billion times below the ones in usual condensed-matter systems. In cold-atom experiments, magnetically tuned scattering resonances (“Feshbach resonances”) serve as a powerful tool to control the two-body coupling strength in the gas (7). Based on such a resonance, a strongly interacting degenerate Fermi gas was recently realized (8). A major breakthrough then followed with the creation of Bose-Einstein condensates of molecular dimers composed of fermionic atoms (9, 10, 11, 12, 13), which corresponds to the realization of a BEC-type superfluid in the strong coupling limit. By variation of the coupling strength, subsequent experiments (14, 15, 16, 12, 17, 18) began to explore the crossover to a BCS-type system. This BEC-BCS crossover

is closely linked to the predicted “resonance superfluidity” (19, 20, 21, 22) and a “universal” behavior of a Fermi gas with resonant interactions (23, 24). The observation of the condensation of atom pairs (15, 16) and measurements of collective oscillations (17, 18) support the expected superfluidity at presently attainable temperatures in Fermi gases with resonant interactions.

Our ultracold gas of fermionic  ${}^6\text{Li}$  atoms is prepared in a balanced spin-mixture of the two lowest sub-states  $|1\rangle$  and  $|2\rangle$  of the electronic  $1s^2 2s$  ground state, employing methods of laser cooling and trapping and subsequent evaporative cooling (9). A magnetic field in the range between 650 to 950 G is applied for Feshbach tuning via a broad resonance centered at  $B_0 \approx 830$  G. In this high-field range, the three lowest atomic levels form a triplet of states  $|1\rangle$ ,  $|2\rangle$ , and  $|3\rangle$ , essentially differing by the orientation of the nuclear spin ( $m_I = 1, 0, -1$ ). In the resonance region with  $B < B_0$ , the s-wave scattering length  $a$  for collisions between atoms in states  $|1\rangle$  and  $|2\rangle$  is positive. Here two-body physics supports a weakly bound molecular state with a binding energy  $E_b = \hbar^2/(ma^2)$ , where  $\hbar$  is Planck’s constant  $h$  divided by  $2\pi$  and  $m$  is the atomic mass. Molecules formed in this state can undergo Bose-Einstein condensation (9, 11, 12, 13). At  $B = B_0$ , the two-body interaction is resonant ( $a \rightarrow \pm\infty$ ) corresponding to a vanishing binding energy of the molecular state. Beyond the resonance ( $B > B_0$ ) the scattering length is negative ( $a < 0$ ), which leads to an effective attraction. Here, two-body physics does not support a weakly bound molecular level and pairing can only occur due to many-body effects.

Our experimental approach (9, 14) facilitates preparation of the quantum gas in various regimes with controlled temperature, Fermi energy, and interaction strength. We perform evaporative cooling under conditions (25) where an essentially pure molecular BEC containing  $N = 4 \times 10^5$  paired atoms can be created as a starting point for the present experiments. The final laser power of the evaporation ramp allows us to vary the temperature  $T$ . The Fermi energy  $E_F$  (Fermi temperature  $T_F = E_F/k_B$  with Boltzmann’s constant  $k_B$ ) is controlled by

a recompression of the gas performed by increasing the trap laser power after the cooling process (25). The interaction strength is then varied by slowly changing the magnetic field to the desired final value. The adiabatic changes applied to the gas after evaporative cooling proceed with conserved entropy (14). Lacking a reliable method to determine the temperature  $T$  of a deeply degenerate, strongly interacting Fermi gas in a direct way, we characterize the system by the temperature  $T'$  measured after an isentropic conversion into the BEC limit (25). For a deeply degenerate Fermi gas, the true temperature  $T$  is substantially below our observable  $T'$  (26, 25), but a general theory for this relation is not yet available.

Radio-frequency (RF) spectroscopy was introduced as a powerful tool to study interaction effects in ultracold Fermi gases (27, 28, 29). Molecular binding energies were measured for  $^{40}\text{K}$  atoms (29), where also the potential of the method to observe fermionic pairing gap energies was pointed out. RF spectroscopy was applied for  $^6\text{Li}$  atoms to study interaction effects up to magnetic fields of 750 G (28). One important observation was the absence of mean-field shifts in the strongly interacting regime. This effect can be attributed to the fact that, in the relevant magnetic-field range, all s-wave scattering processes between  $^6\text{Li}$  atoms in the states  $|1\rangle$ ,  $|2\rangle$  and  $|3\rangle$  are simultaneously unitarity limited. This property of  $^6\text{Li}$  is very favorable for RF spectroscopy as it suppresses shifts and broadening by mean-field effects.

We drive RF transitions from state  $|2\rangle$  to the empty state  $|3\rangle$  at  $\sim 80$  MHz, and monitor the loss of atoms in state  $|2\rangle$  after weak excitation by a 1-s RF pulse, using state-selective absorption imaging (14). Our experiment is optimized to obtain a resolution of  $\sim 100$  Hz, corresponding to an intrinsic sensitivity to interaction effects on the scale of  $\sim 5$  nK, which is more than two orders of magnitude below the typical Fermi temperatures.

We recorded RF spectra for different degrees of cooling and in various coupling regimes (Fig. 1). We realize the molecular regime at  $B = 720$  G ( $a = +120$  nm). For the resonance region, we examined two different magnetic fields because the precise resonance location  $B_0$  is

not exactly known. Our two values  $B = 822 \text{ G}$  (16) and  $837 \text{ G}$  (13, 18) may be considered as lower and upper bounds for  $B_0$ . We also studied the regime beyond the resonance with large negative scattering length at  $B = 875 \text{ G}$  ( $a \approx -600 \text{ nm}$ ). Spectra taken in a “hot” thermal sample at  $T \approx 6T_F$  ( $T_F = 15 \mu\text{K}$ ) show the narrow atomic  $|2\rangle \rightarrow |3\rangle$  transition line (upper row in Fig. 1) and serve as a frequency reference. We present our spectra as a function of the RF offset with respect to the bare atomic transition frequency.

Spectral signatures of pairing have been theoretically considered (30, 31, 32, 33, 34). A clear signature of the pairing process is the emergence of a double-peak structure in the spectral response as a result of the coexistence of unpaired and paired atoms. The pair-related peak is located at a higher frequency than the unpaired-atoms signal as energy is required for pair breaking. For understanding the spectra both the homogeneous lineshape of the pair signal (31, 33) and the inhomogeneous line broadening due to the density distribution in the harmonic trap need to be taken into account (34). As an effect of inhomogeneity, fermionic pairing due to many-body effects takes place predominantly in the central high-density region of the trap, and unpaired atoms mostly populate the outer region of the trap where the density is low (35, 36, 34). The spectral component corresponding to the pairs thus shows a large inhomogeneous broadening in addition to the homogeneous width of the pair-breaking signal. For the unpaired atoms the homogeneous line is narrow and the effects of inhomogeneity and mean-field shifts are negligible. These arguments explain why the RF spectra in general show a relatively sharp peak for the unpaired atoms together with a broader peak attributed to the pairs.

We observe clear double-peak structures already at  $T'/T_F = 0.5$ , which we obtain with moderate evaporative cooling down to a laser power of  $P = 200 \text{ mW}$  (middle row in Fig. 1,  $T_F = 3.4 \mu\text{K}$ ). In the molecular regime ( $B = 720 \text{ G}$ ), the sharp atomic peak is well separated from the broad dissociation signal (29), which shows a molecular binding energy of  $E_b = h \times 130 \text{ kHz} = k_B \times 6.2 \mu\text{K}$ . For  $B$  approaching  $B_0$ , the peaks begin to overlap. In the resonance

region (822 and 837 G), we still observe a relatively narrow atomic peak at the original position together with a pair signal. For magnetic fields beyond the resonance, we can resolve the double-peak structure for fields up to  $\sim 900$  G.

For  $T'/T_F < 0.2$ , realized with a deep evaporative cooling ramp down to an optical trap power of  $P = 3.8$  mW, we observe a disappearance of the narrow atomic peak in the RF spectra (lower row in Fig. 1,  $T_F = 1.2\mu\text{K}$ ). This shows that essentially all atoms are paired. In the BEC limit (720 G) the dissociation lineshape is identical to the one observed in the trap at higher temperature and Fermi energy. Here the localized pairs are molecules with a size much smaller than the mean interparticle spacing, and the dissociation signal is independent of the density. In the resonance region (822 and 837 G) the pairing signal shows a clear dependence on density (Fermi energy), which becomes even more pronounced beyond the resonance (875 G). We attribute this to the fact that the size of the pairs becomes comparable to or larger than the interparticle spacing. In addition, the narrow width of the pair signal in this regime (lower row in Fig. 1,  $B = 875$  G) indicates a pair localization in momentum space to well below the Fermi momentum  $\hbar k_F = \sqrt{2mE_F}$  and thus a pair size exceeding the interparticle spacing.

To quantitatively investigate the crossover from the two-body molecular regime to the fermionic many-body regime we measure the pairing energy in a range between 720 G and 905 G. The measurements were performed after deep evaporative cooling ( $T'/T_F < 0.2$ ) for two different Fermi temperatures  $T_F = 1.2\mu\text{K}$  and  $3.6\mu\text{K}$  (Fig. 2). As an effective pairing gap we define  $\Delta\nu$  as the frequency difference between the pair-signal maximum and the bare atomic resonance. In the BEC limit, the effective pairing gap  $\Delta\nu$  simply reflects the molecular binding energy  $E_b$  (solid line in Fig. 2) (25). With increasing magnetic field, in the BEC-BCS crossover,  $\Delta\nu$  shows an increasing deviation from this low-density molecular limit and smoothly evolves into a density-dependent many-body regime where  $\hbar\Delta\nu < E_F$ .

A comparison of the pairing energies at the two different Fermi energies (inset in Fig. 2)

provides further insight into the nature of the pairs. In the BEC limit,  $\Delta\nu$  is solely determined by  $E_b$  and thus does not depend on  $E_F$ . In the universal regime on resonance,  $E_F$  is the only energy scale and we indeed observe the effective pairing gap  $\Delta\nu$  to increase linearly with the Fermi energy. We find a corresponding relation  $h\Delta\nu \approx 0.2 E_F$ . Beyond the resonance, where the system is expected to change from a resonant to a BCS-type behavior,  $\Delta\nu$  is found to depend more strongly on the Fermi energy and the observed gap ratio further increases. We interpret this in terms of the increasing BCS character of pairing, for which an exponential dependence  $h\Delta\nu/E_F \propto \exp(-\pi/2k_F|a|)$  is expected.

In a further series of measurements (Fig. 3), we applied a controlled heating method to study the temperature dependence of the gap in a way which allowed us to keep all other parameters constant. After production of a pure molecular BEC ( $T' < 0.2T_F$ ) in the usual way, we adiabatically changed the conditions to  $B = 837$  G and  $T_F = 1.2 \mu\text{K}$ . We then increased the trap laser power by a factor of nine ( $T_F$  increased to  $2.5 \mu\text{K}$ ) using exponential ramps of different durations. For fast ramps this recompression is non-adiabatic and increases the entropy. By variation of the ramp time, we explore a range from our lowest temperatures up to  $T'/T_F = 0.8$ . The emergence of the gap with decreasing temperature is clearly visible in the RF spectra (Fig. 3). The marked increase of  $\Delta\nu$  for decreasing temperature is in good agreement with theoretical expectations for the pairing gap energy (5).

The situation of our experiment was theoretically analyzed for the case of resonant two-body interaction (34). The calculated RF spectra are in agreement with our experimental results and demonstrate how a double-peak structure emerges as the gas is cooled below  $T/T_F \approx 0.5$  and how the atomic peak disappears with further decreasing temperature. In particular, the work clarifies the role of the “pseudo-gap” regime (5, 22), in which pairs are formed before superfluidity is reached. According to the calculated spectra, the atomic peak disappears at temperatures well below the critical temperature for the phase-transition to a superfluid. A

recent theoretical study of the BCS-BEC crossover at finite temperature (36) predicts the phase-transition to a superfluid to occur at a temperature that on resonance is only  $\sim 30\%$  below the point where pair formation sets in.

We have observed fermionic pairing already after moderate evaporative cooling. With much deeper cooling applied, the unpaired atom signal disappeared from our spectra. This observation shows that pairing takes place even in the outer region of the trapped gas where the density and the local Fermi energy are low. Our results thus strongly suggest that a resonance superfluid is formed in the central region of the trap (34). Together with the observations of resonance condensation of fermionic pairs (15, 16) and weak damping of collective excitations (17, 18), our observation of the pairing gap provides a strong case for superfluidity in present experiments on resonantly interacting Fermi gas.



## References and Notes

1. M. Tinkham, *Introduction to Superconductivity*, second edition (McGraw-Hill, New York, 1996).
2. D. M. Eagles, Phys. Rev. **186**, 456 (1969).
3. A. J. Leggett, in *Modern Trends in the Theory of Condensed Matter*, edited by A. Pekalski and R. Przystawa (Springer-Verlag, Berlin, 1980), pp. 13-27.
4. P. Nozières, S. Schmitt-Rink, J. Low Temp. Phys. **59**, 195 (1985).
5. Q. Chen, J. Stajic, S. Tan and K. Levin, preprint available at <http://arxiv.org/abs/cond-mat/0404274>.
6. See News Focus article by A. Cho, *Science* **301**, 750 (2003).
7. S. Inouye *et al.*, Nature **392**, 151 (1998).
8. K. M. O'Hara, S. L. Hemmer, M. E. Gehm, S. R. Granade, J. E. Thomas, *Science* **298**, 2179 (2002); published online 7 Nov 2002 (10.1126/science.1079107).
9. S. Jochim *et al.*, *Science* **302**, 2101 (2003); published online November 13, 2003 (10.1126/science.1093280).
10. M. Greiner, C. A. Regal, D. S. Jin, Nature **426**, 537 (2003).
11. M. W. Zwierlein *et al.*, Phys. Rev. Lett. **91**, 250401 (2003).
12. T. Bourdel *et al.*, preprint available at <http://arxiv.org/abs/cond-mat/0403091>.
13. R. Hulet, KITP Conference on Quantum Gases, Santa Barbara, May 10 - 14, 2004.

14. M. Bartenstein *et al.*, Phys. Rev. Lett. **92**, 120401 (2004).
15. C. A. Regal, M. Greiner, D. S. Jin, Phys. Rev. Lett. **92**, 040403 (2004).
16. M. W. Zwierlein *et al.*, Phys. Rev. Lett. **92**, 120403 (2004).
17. J. Kinast, S. L. Hemmer, M. E. Gehm, A. Turlapov, J. E. Thomas, Phys. Rev. Lett. **92**, 150402 (2004).
18. M. Bartenstein *et al.*, Phys. Rev. Lett. **92**, 203201 (2004).
19. M. Holland, S.J.J.M.F. Kokkelmans, M. L. Chiofalo, R. Walser, Phys. Rev. Lett. **87**, 120406 (2001).
20. E. Timmermans, K. Furuya, P. W. Milonni, A. K. Kerman, Phys. Lett. A **285**, 228 (2001).
21. Y. Ohashi, A. Griffin, Phys. Rev. Lett. **89**, 130402 (2002).
22. J. Stajic *et al.*, Phys. Rev. A **69**, 063610 (2004).
23. H. Heiselberg, Phys. Rev. A **63**, 043606 (2001).
24. T.-L. Ho, Phys. Rev. Lett. **92**, 090402 (2004).
25. Materials and methods are available as supporting material on *Science Online*.
26. L. D. Carr, G. V. Shlyapnikov, Y. Castin, Phys. Rev. Lett. **92**, 150404 (2004).
27. C. Regal, D. Jin, Phys. Rev. Lett. **90**, 230404 (2003).
28. S. Gupta *et al.*, Science **300**, 1723 (2003); published online May 8, 2003 (10.1126/science.1085335).
29. C. A. Regal, C. Ticknor, J. L. Bohn, D. S. Jin, Nature **424**, 47 (2003).

30. P. Törmä, P. Zoller, Phys. Rev. Lett. **85**, 487 (2000).
31. J. Kinnunen, M. Rodriguez, P. Törmä, Phys. Rev. Lett. **92**, 230403 (2004).
32. H. P. Büchler, P. Zoller, W. Zwerger, preprint available at <http://arxiv.org/abs/cond-mat/0404116>.
33. R. B. Diener, T.-L. Ho, preprint available at <http://arxiv.org/abs/cond-mat/0405174>.
34. J. Kinnunen, M. Rodriguez, P. Törmä, preprint available at <http://arxiv.org/abs/cond-mat/0405633>.
35. A. Bulgac, preprint available at <http://arxiv.org/abs/cond-mat/0309358>.
36. A. Perali, P. Pieri, L. Pisani, G. C. Strinati, Phys. Rev. Lett. **92**, 220404 (2004).
37. We thank P. Törmä for a stimulating exchange of results and very useful discussions. We thank W. Zwerger and H.P. Büchler for many stimulating discussions. We acknowledge support by the Austrian Science Fund (FWF) within SFB 15 (project part 15) and by the European Union in the frame of the Cold Molecules TMR Network under Contract No. HPRN-CT-2002-00290. C.C. is a Lise-Meitner research fellow of the FWF.

### **Supporting Online Material**

[www.sciencemag.org](http://www.sciencemag.org)

Materials and Methods

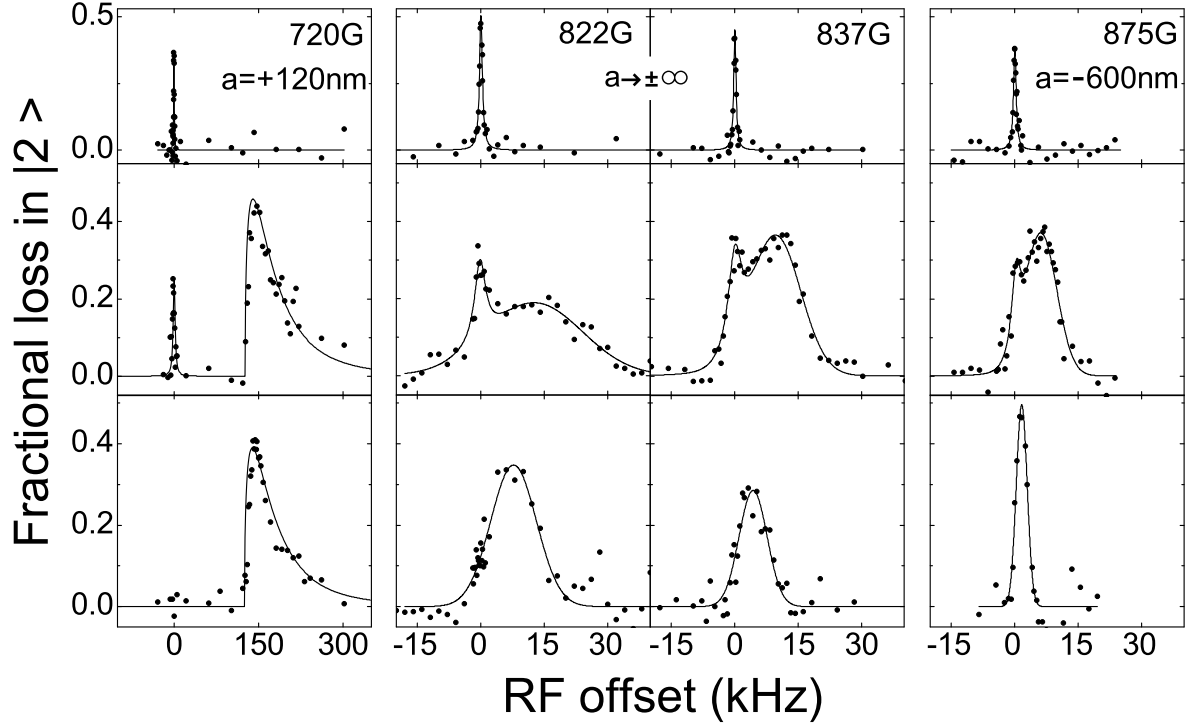


**Fig. 1.** RF spectra for various magnetic fields and different degrees of evaporative cooling. The RF offset ( $k_B \times 1 \mu\text{K} \simeq h \times 20.8 \text{ kHz}$ ) is given relative to the atomic transition  $|2\rangle \rightarrow |3\rangle$ . The molecular limit is realized for  $B = 720 \text{ G}$  (first column). The resonance regime is studied for  $B = 822 \text{ G}$  and  $837 \text{ G}$  (second and third column). The data at  $875 \text{ G}$  (fourth column) explore the crossover on the BCS side. Upper row, signals of unpaired atoms at  $T' \approx 6T_F$  ( $T_F = 15 \mu\text{K}$ ); middle row, signals for a mixture of unpaired and paired atoms at  $T' = 0.5T_F$  ( $T_F = 3.4 \mu\text{K}$ ); lower row, signals for paired atoms at  $T' < 0.2T_F$  ( $T_F = 1.2 \mu\text{K}$ ). Note that the true temperature  $T$  of the atomic Fermi gas is below the temperature  $T'$  which we measure in the BEC limit (see text). The solid lines are introduced to guide the eye.

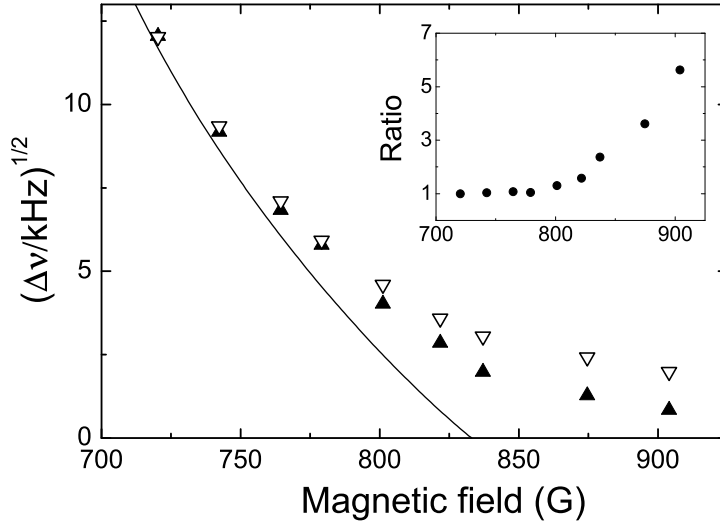


**Fig. 2.** Measurements of the effective pairing gap  $\Delta\nu$  as a function of the magnetic field  $B$  for deep evaporative cooling and two different Fermi temperatures  $T_F = 1.2\mu\text{K}$  (filled symbols) and  $3.6\mu\text{K}$  (open symbols). The solid line shows  $\Delta\nu$  for the low-density limit where it is essentially given by the molecular binding energy (25). The inset displays the ratio of the effective pairing gaps measured at the two different Fermi energies.

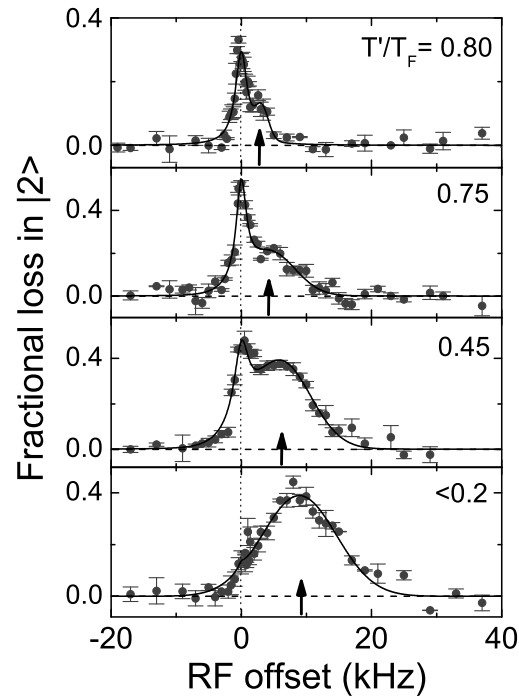


**Fig. 3.** RF spectra measured at  $B = 837\text{ G}$  and  $T_F = 2.5\ \mu\text{K}$  for different temperatures  $T'$  adjusted by controlled heating. The solid lines are fits to guide the eye using a Lorentzian curve for the atom peak and a Gaussian curve for the pair signal. The vertical dotted line marks the atomic transition and the arrows indicate the effective pairing gap  $\Delta\nu$ .

# Observation of the Pairing Gap in a Strongly Interacting Fermi Gas

*C. Chin, M. Bartenstein, A. Altmeyer, S. Riedl, S. Jochim,  
J. Hecker Denschlag, R. Grimm*

## Materials and Methods

### Evaporative cooling, trap frequencies and Fermi energy

Our optical dipole trap consists of a single laser beam (wavelength 1030 nm) focused to a waist of  $25\mu\text{m}$ . Evaporative cooling is performed at a magnetic field of  $B = 764\text{ G}$  by exponentially decreasing the trap laser power  $P$  from initially 10.5 W, with a fixed time constant of 460 ms, down to a variable final power. About  $2 \times 10^6$  atoms are initially loaded into the trap. After the full evaporation ramp down to a final power of 3.8 mW,  $N/2 = 2 \times 10^5$  molecules ( $N = 4 \times 10^5$  atoms) are left in the trap.

The radial and axial trap frequencies  $\omega_r, \omega_z$  are measured as a function of the laser power  $P$  and described by

$$\begin{aligned}\omega_r/2\pi &= 127\text{ Hz} \times (P/\text{mW})^{1/2}, \\ \omega_z/2\pi &= (601B/\text{kG} + 0.3P/\text{mW})^{1/2}\text{Hz}.\end{aligned}$$

At low laser power, the axial confinement is dominated by the curvature of the magnetic field used for Feshbach tuning.

The Fermi energy  $E_F = \hbar(3\omega_r^2\omega_z N)^{1/3}$  for a non-interacting gas is calculated from the trap frequencies and the measured number  $N$  of paired and unpaired atoms in both internal states.

### Thermometry

To characterize the entropy of the gas we use the temperature  $T'$  that is measured after an adiabatic and reversible (i.e. isentropic) conversion of the gas into the BEC limit. In this regime better thermometry is available than in the crossover region. We determine  $T'$  at a magnetic field of 676 G by fitting the well-known bimodal distribution to *in-situ* images of the trapped, partially condensed molecular cloud [S1]. For the full evaporation ramp, we observe a condensate fraction of  $>90\%$ . From this lower limit for the condensate fraction (taking into account

interaction effects) we determine an upper limit for the temperature  $T'/T_{\text{BEC}} < 0.4$ , where the critical temperature  $T_{\text{BEC}}$  for a non-interacting molecular BEC of  $M = N/2$  dimers is given by  $k_B T_{\text{BEC}} = \hbar(\omega_r^2 \omega_z M / 1.202)^{1/3}$ . Using the relation  $T_{\text{BEC}} = 0.518 T_F$  for a two-component Fermi gas in a harmonic trap, we rewrite the temperature in terms of the Fermi energy and we finally obtain  $T' < 0.2 T_F$  for our deep evaporative cooling conditions.

For the relation of the true temperature  $T$  in the crossover region to our observable  $T'$ , a general theory is presently not available. However, it was theoretically shown that the isentropic conversion of a molecular BEC with  $T'/T_F \ll 1$  to a non-interacting Fermi gas leads to a strong temperature reduction, following a scaling  $T/T_F \propto (T'/T_F)^3$  [S2]. In a similar way, we can also expect a substantial temperature reduction when the molecular BEC is converted into a strongly interacting gas with resonant interactions.

## Experimental details for Figures 1-3

**Fig. 1:** The measurements shown in the three rows are taken for different evaporative cooling and adiabatic recompression conditions. The relevant parameters are summarized in the following table:

	final evap. power	$N$	recompression	$T_F$
upper row: no evaporation	10.5 W (no ramp)	$2 \times 10^6$	10.5 W (no ramp)	$15 \mu\text{K}$
middle row: moderate evap.	200 mW	$1.0 \times 10^6$	310 mW	$3.4 \mu\text{K}$
lower row: deep evaporation	3.8 mW	$4 \times 10^5$	34 mW	$1.2 \mu\text{K}$

**Fig. 2:** All measurements are taken with  $N = 4 \times 10^5$  atoms after full evaporative cooling down to a laser power of 3.8 mW (same as in the lower row of Fig 1). The filled symbols refer to the case of a subsequent recompression to  $P = 34\text{mW}$  corresponding to  $T_F = 1.2 \mu\text{K}$ , and the open symbols refer to a recompression to  $P = 930\text{mW}$  corresponding to  $T_F = 3.6 \mu\text{K}$ .

**Fig. 3:** Full evaporation with same parameters as in the lower row of Fig. 1 and in Fig. 2. After evaporation, the trap power is increased to  $P = 310\text{mW}$  yielding  $T_F = 2.5 \mu\text{K}$  for  $N = 4 \times 10^5$  atoms. The recompression is performed adiabatically (lower picture) or rapidly with different time constants to implement controlled heating.

RF power: In all measurements, we individually adjust the RF power to obtain a maximum loss of  $\sim 40\%$  in state  $|2\rangle$ . This value is chosen as a compromise between good signal-to-noise ratio and minimum perturbation of the system. The RF is generally weak and applied to the sample for a long time of 1 s to avoid broadening effects.



## RF molecular dissociation lineshape in low-density limit

The radio-frequency  $\nu_{\text{RF}}$  couples the atomic states  $|2\rangle$  and  $|3\rangle$ . For a non-interacting atomic gas, the transition frequency  $\nu_{23}$  as a function of the magnetic field  $B$  is determined by the well-known Breit-Rabi formula. In the magnetic-field range of interest the nuclear spin almost decouples from the electron spin (Paschen-Back regime) and  $\nu_{23}$  is about 80 MHz. We introduce  $\delta\nu_{\text{RF}} = \nu_{\text{RF}} - \nu_{23}$  as the RF offset from the atomic resonance.

In the case of a weakly bound molecule, formed with a binding energy  $E_b$  by an atom in state  $|1\rangle$  and an atom in state  $|2\rangle$ , the RF can dissociate the molecule if the threshold condition  $h\delta\nu_{\text{RF}} > E_b$  is fulfilled. Above threshold, the RF-induced dissociation produces two atoms with a total kinetic energy of  $2E_k$ . In the center-of-mass system, where the molecule is at rest, energy conservation reads

$$h\delta\nu_{\text{RF}} = E_b + 2E_k.$$

The lineshape of the continuous RF dissociation signal can be understood in terms of the Franck-Condon overlap of the molecular wave function with the wavefunction in the dissociation channel (a pair of atoms in the states  $|1\rangle$  and  $|3\rangle$ ). The wavefunction of the molecule (dimer of atoms in  $|1\rangle$  and  $|2\rangle$ ) is essentially determined by the scattering length  $a$  (or the corresponding binding energy  $E_b \approx \hbar^2/ma^2$ ). The dissociation-channel wavefunction in general depends on the kinetic energy  $E_k$  and the scattering length  $a_{13}$ . For  $a \ll |a_{13}|$ , we find that the dependence on  $a_{13}$  has negligible influence on the lineshape. However, for  ${}^6\text{Li}$  the dissociation channel exhibits a broad Feshbach resonance at  $\sim 690$  G, which significantly affects our dissociation lineshape. A calculation of the lineshape [S3] yields the expression

$$f(E) \propto E^{-2}(E - E_b)^{1/2}(E - E_b + E')^{-1}$$

where  $E = h\delta\nu_{\text{RF}}$  and  $E' = \hbar^2/ma_{13}^2$ .

According to our definition, the effective pairing gap  $h\Delta\nu$  in the low-density molecular limit is directly given by the maximum of the molecular dissociation signal. From the above lineshape  $f(E)$  it is straightforward to calculate the signal maximum

$$h\Delta\nu = \xi E_b,$$

where  $\xi$  weakly depends on  $E'/E_b$  and varies between the two limits  $\xi = 1$  and  $\xi = 4/3$  for  $E' \ll E_b$  and  $E' \gg E_b$ , respectively.

The magnetic-field dependence of  $\Delta\nu$  that we show as solid line in Fig. 2 is calculated on the basis of the above lineshape  $f(E)$  and the most recent data for the scattering lengths  $a$  and  $a_{13}$  (and the corresponding energies  $E_b$  and  $E'$ ) from the NIST group [S4].

## References

- S1. M. Bartenstein et al., *Phys. Rev. Lett.* **92**, 203201 (2004).
- S2. L. D. Carr, G. V. Shlyapnikov, Y. Castin, *Phys. Rev. Lett.* **92**, 150404 (2004).
- S3. C. Chin, P. Julienne, to be published.
- S4. P. Julienne, A. Simoni, E. Tiesinga, private communication.